INTERNATIONAL JOURNAL OF COMMUNICATION SYSTEMS
Int. J. Commun. Syst. 2014; **00**:1–18
Published online in Wiley InterScience (www.interscience.wiley.com). DOI: 10.1002/dac

Performance Analysis of Distributed Underwater Wireless Acoustic Sensor Networks Systems in the Presence of Internal Solitons

A. K. Mandal[1], S. Misra[2*], M. K. Dash[3], T. Ojha[4]

[1,2,4]*School of Information Technology*
[1,3]*Center for Oceans, Rivers, Atmospheric and Land Sciences*
Indian Institute of Technology, Kharagpur - 721302
Email: [1]*amiit.mandal@gmail.com,* [2]*smisra@sit.iitkgp.ernet.in,* [3]*mihir@coral.iitkgp.ernet.in* [4]*tojha@sit.iitkgp.ernet.in*

SUMMARY

In this paper, we have analyzed the performance of distributed Underwater Wireless Acoustic Sensor Networks (UWASNs) in the presence of internal solitons in the ocean. Internal waves commonly occur in a layered oceanic environment having differential medium density. So, in a layered shallow oceanic region, the inclusion of the effect of internal solitons on the performance of the network is important. Based on various observations, it is proved that non-linear internal waves, i.e., solitons are one of the major scatterers of underwater sound. If sensor nodes are deployed in such type of environment, inter-node communication is affected due to the interaction of wireless acoustic signal with these solitons, as a result of which network performance is greatly affected. We have evaluated the performance of UWASNs in the 3-D deployment scenario of nodes, in which source nodes are deployed in the ocean floor. In this paper, four performance metrics, namely, Signal-to-interference-plus-noise-ratio (SINR), Bit error rate (BER), Delay (DELAY), and energy consumption are introduced to assess the performance of UWASNs. Simulation studies show that in the presence of internal solitons, SINR decreases by approximately 10 %, BER increases by 17 %, delay increases by 0.24 %, and energy consumption per node increases by 53.05 %, approximately.

Received . . .

KEY WORDS: Distributed underwater sensor networks, acoustic communication, internal soliton, acoustics signal, scattering

1. INTRODUCTION

This paper presents the performance analysis of distributed UWASN systems in the presence of internal solitons, which commonly occur in shallow coastal oceanic environments having differential medium density. UWASNs can be used to collect oceanographic data, monitor pollution, prevent disaster, and for tactical surveillance applications [1], [2], [3], [4].

Unlike the communication channel in terrestrial wireless sensor networks, which is mostly static in nature, underwater communication channel is much more dynamic [5]. This dynamism arises due to the non-uniform distribution of different physical parameters. There are various existing literature (e.g., [6], [7], [8], [9], [10], [11], [12]) on UWASNs. However, they have ignored the effect of solitons on the network performance.

*Correspondence to: School of Information Technology, Indian Institute of Technology, Kharagpur - 721302. Email: smisra@sit.iitkgp.ernet.in
†This work is partially supported by a grant from the Department of Electronics and Information Technology, Government of India, Grant No. 13(10)/2009-CC-BT, which the authors gratefully acknowledge.

A UWASN is formed of sensor nodes deployed in some region of the ocean and they communicate with one another through wireless mode using acoustic signals [13][14]. The characteristics of the deployment region varies both spatially and temporally. Some regions are prone to more naturally occurring more dynamic oceanic phenomena than others. In those regions communication performance is affected due to the inter-node link quality degradation caused by the interaction of acoustic signal with the dynamic oceanic physical phenomenon. One such phenomenon having strong influence on acoustic signal propagation is internal soliton, which arises in a stratified oceanic environment, typically in shallow water region of depth limited by 200 m. A strong internal wave, which is non-linear in nature, is known as an internal soliton, and it advances in packet form through the *ocean column*. Solitons are well-known in acoustics as sound scatterers [15]. They affect the acoustic signal of frequency, f, in the range $1\,kHz \leq f \leq 50\,kHz$, which is the optimum frequency range of inter-node communication in UWASNs.

In the soliton-induced region, the wireless acoustic link quality is perturbed by the existence of soliton wave packets. The creation of solitons depends on both intrinsic dispersion and non-linearity of the medium. In shallow water regions, internal solitons are often strongly non-linear in nature [15]. They mainly affect the upper or shallow coastal regions of an ocean.

2. RELATED WORK AND CONTRIBUTION

There exists works (e.g. [16][17][18]) on the study of performance of terrestrial wireless sensor network under different scenarios. Unlike terrestrial wireless sensor network, UWASNs are subjected to increased challenges due to adverse conditions of underwater channel. Again, compared to deep water, shallow water is prone to increased dynamism. Therefore, it is important to assess the performance of UWASNs in shallow underwater regions.

There are works (e.g., [19] [20]) specifically on shallow underwater acoustic networks, and generally on UWASNs, such as [21] [22]. Particularly, from the perspective of UWASNs, performance evaluation in the physical layer was undertaken on various aspects. Most of these pieces of work are focused on the physical characteristics of acoustic signal. There is lack of work on the performance evaluation of UWASNs in the presence of waves existing inside the water body of the ocean.

Ismail et al. [23] assessed the performance of UWASNs on the basis of signal attenuation through oceanic under water columns only. In [24], Zorzi et al. have taken linear topologies of sensor nodes and considered noise, propagation delay, and their impacts on the transmission power and bandwidth. They have not considered any realistic dynamic phenomena existing in the channel. Stefanov and Stojanovic [25] analyzed interference induced performance analysis of wireless acoustic networks. They modeled frequency dependent path loss of acoustic signals connecting nodes using the wireless mode of communication. The research work does not consider any realistic physically occurring oceanic phenomenon in the channel. In [26], Babu et al. have considered the frequency dependent fading and time variation characteristics of underwater channel. However, they have not considered the any underwater dynamic phenomenon like internal solitons. Xu et al. [27] evaluated the performance of UWASNs by considering different metrics such as packet delivery ratio, network throughput, energy consumption, and end-to-end delay. However, performance evaluation was executed in the presence of node mobility and other common aspects relevant to underwater channel. They have not considered any dynamic underwater phenomena, occurred in the ocean. In addition to considering the commonly reported problems in underwater such as delay, path loss, and Doppler spread [28], Ancy et al. have also shown the technique of data transmission in the presence of shadow zone. However, they did not consider any dynamical phenomenon in the channel through which data transmission takes place. Llor et al. [29] analyzed the transmission loss of signals for UWASNs by considering the environmental factors such as surface waves. However, they have not considered any phenomenon governing the volume of water. Xie et al. [30] statistically modeled the path loss between two sensor nodes at a particular frequency and time. In predicting the path loss of an acoustic signal in underwater, they have only considered the surface wave activity on the movement of sensor nodes.

DOI: 10.1002/dac

From the review of existing literature, it can be inferred that the effect of internal solitons on the communication performance has not been studied so far. In our work, we have considered the existence of internal solitons in shallow oceanic coastal region, and have studied their effect on the performance of UWASNs.

3. ANALYTICAL CHARACTERIZATION OF INTERNAL SOLITONS

Internal solitons are ubiquitous in coastal oceanic water having stratified layered column. In this section, we briefly introduce their analytical characteristics and dynamics.

3.1. Characteristics of internal soliton

Internal solitons propagate along the pycnocline of a ocean. However, their generation can be achieved in different ways such as direct displacement of pycnocline, and conversion of complex tidal energy into the pycnocline motion. The interaction of internal tide with the irregular bottom topography leads to the formation of internal solitons. As their names imply, they propagate through the interior of the ocean. Solitary waves are a class of non-sinusoidal, non-linear, mostly isolated waves of complex shape occurring frequently in nature [31]. Internal solitons consist of several oscillations confined in a particular region or space. They always remain in packet form and can carry considerable shear velocity leading to turbulence and mixing. This mixing often introduces bottom nutrients of ocean to the upper part in it. They play a significant role in the dynamics of shallow oceanic coastal zone as well as deep water zone [32]. They are mostly found in the shelf region of an ocean, and have significant impact on the acoustical properties in shallow coastal area.

In our work, we consider UWASNs deployed in the shallow coastal zone of an ocean. Therefore, it is important to understand the characteristics of internal solitons affecting the communication performance of the whole network. The following are the characteristics of internal solitons:

- The solitons in shallow water regions are usually observed in packet form. They are also known as solitary waves. In particular, they are observed during summer when they are trapped in strong seasonal thermocline [33].
- The solitons in shallow water are described by the Korteweg-de Vries equation [15], which is explained in this Section briefly. These solitons exist in the rank order.
- The wave packets are highly co-related. Maximum number of packets occurs during the spring tide and minimum number occur during the neap tide [33]. After formation, they propagate shoreward and their variation is also observed due to the change in bottom topography.
- Their surface signature is mainly observed in summer season due to the shift of thermocline towards surface.

3.2. Governing equations

For an incompressible stratified fluid in a gravity field, the hydrodynamical equations are given as [34]:

$$\frac{d\vec{U}}{dt} + \frac{1}{\rho}\vec{\nabla}p = -f(\hat{k} \times \vec{U}) - \vec{g} \tag{1}$$

$$\frac{\partial \rho}{\partial t} + (\vec{\nabla}.\vec{U})\rho = 0 \tag{2}$$

$$\vec{\nabla}.\vec{U} = 0 \tag{3}$$

In Equation (1), $\vec{U} = (u_x, u_y, u_z)$ is the velocity vector of a fluid parcel, p is the fluid pressure, $\vec{g}$ is the gravitational acceleration, $\hat{k}$ is the unit vector acting vertically upward along the increasing +z direction, and $f = 2\,\Omega\, sin\phi$ is the Coriolis parameter, where, Ω and ϕ are, respectively, the Earth's angular velocity of rotation, and geographical latitude of a particular place on the Earth.

Due to the presence of internal waves, density perturbation occurs. Using the Boussineq

DOI: 10.1002/dac

approximation, we can write the density field in the presence of internal waves as:

$$\rho = \rho_0(z) + \rho_{per}(x, y, z, t), \quad \rho_{per} \ll \rho_0 \tag{4}$$

In Equation (4), ρ_0 is the equilibrium or unperturbed depth dependent density, and ρ_{per} is the perturbed density. As per Boussineq's approximation, vertical variation of $\rho_0(z)$ is significant for only the buoyancy term, which is proportional to $\frac{d\rho_0}{dz}$ [15]. Let the shallow water region be bounded by two surfaces, z = 0 and z = -D, where D is the depth in meters. Zero vertical displacement is applied at these two surfaces.

Using Boussineq approximation, the hydrodynamical equations in presence of internal waves can be written as [35]:

$$\vec{\nabla}.\vec{U_h} + \frac{\partial u_z}{\partial z} = 0 \tag{5}$$

$$\frac{\partial \vec{U_h}}{\partial t} + \frac{1}{\rho_0}\vec{\nabla}p^{'} + \rho_0 f(\hat{k} \times \vec{U_h}) + (u_z\frac{\partial \vec{U_h}}{\partial z} + (\vec{\nabla}.\vec{U_h})U_h) = 0 \tag{6}$$

$$\frac{\partial \rho^{'}}{\partial t} + u_z\frac{d\rho_0}{dz} + (u_z\frac{\partial \rho^{'}}{\partial z} + (\vec{\nabla}.\vec{U_h})\rho^{'}) = 0 \tag{7}$$

$$\frac{\partial p^{'}}{\partial t} + g\rho^{'} + (u_z\frac{\partial u_z}{\partial z} + (\vec{\nabla}.\vec{U_h})u_z) + \rho_0\frac{\partial u_z}{\partial t} = 0 \tag{8}$$

In Equations (5) – (8), $\vec{U_h} = (u_x, u_y)$ is the velocity vector existing in the x-y plane and the operator $\vec{\nabla}$ is a two dimensional one, which is as:

$$\vec{\nabla} = \hat{i}\frac{\partial}{\partial x} + \hat{j}\frac{\partial}{\partial y} \tag{9}$$

3.3. Theoretical model for shallow water internal solitons

Tidal interaction with the ocean bottom topography appears to be the dominant mechanism for the generation of coherent internal waves near the continents [15]. It is well known that acoustic transmission loss depends strongly on frequency. Again, the results of experiments reported in the literature [36]-[33] show that wireless acoustic communication is affected due to acoustic signal scattering over various frequency ranges by solitons arising due to vertical (upward and downward) displacement of the pycnocline layer under the combined effect of buoyancy force and gravitational force. Therefore, while sensor network is deployed in such internal solitons induced region, inter-node wireless acoustic communication is affected.

We expand the vertical velocity, u_z, and the horizontal velocity, $\vec{U_h}$, in terms of eigenmodes. The eigenmode representation of these two terms are as follows:

$$u_z = \sum_{n=1}^{\infty}(U_z)_n(u_z)_n(x, y, t) \tag{10}$$

$$\vec{U_h} = \sum_{n=1}^{\infty}\kappa_n\frac{d(U_z)_n}{dz}(u_h)_n(x, y, t) \tag{11}$$

In Equations (10) and (11), n is the mode number, $(U_z)_n$ denotes the orthogonal eigen functions, and κ_n is a constant. The vertical displacement, η, of an isopycnal surface is represented as:

$$\eta(\vec{r}, t) = \sum_{n=1}^{\infty}\eta_n(x, y, t)(U_z)_n \tag{12}$$

DOI: 10.1002/dac

Under the non-dispersive and linear approximation, the function $(U_z)_n$ satisfies the following second order differential equation as:

$$\frac{d^2U_z}{dz^2} + \frac{N^2}{c^2}U_z = 0 \tag{13}$$

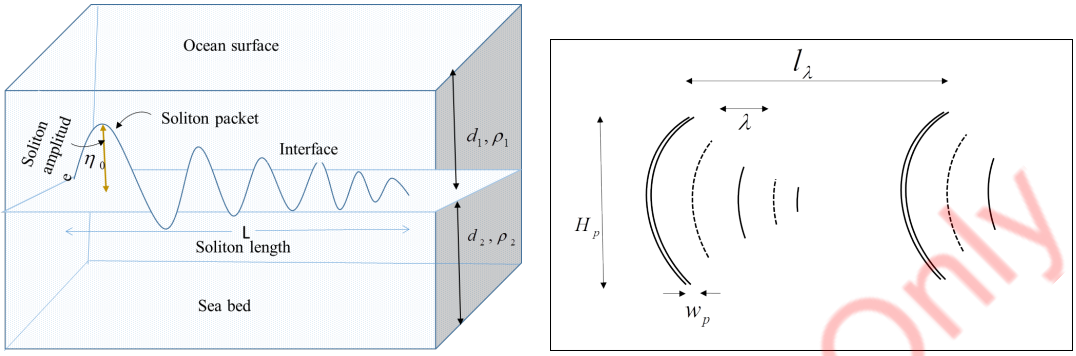

(a) Generation of internal wave in shallow water

(b) Horizontal view of the advancement of solitons in the ocean

Figure 1. Schematic view of generation and propagation of internal solitons in shallow coastal ocean

In Equation (13), the quantity N is known as the Brunt-Väisälä frequency, which is in the order of 10 cycles/hr. It is expressed in terms of rad/sec. When $N^2>0$, the water column is stably stratified. It is expressed as:

$$N = \sqrt{-\frac{g}{\rho_0}\frac{d\rho_0}{dz}} \tag{14}$$

With this frequency, N, a stably stratified column of water oscillates under the combined influence of gravity and buoyancy forces. Figure 1 shows a two layered internal wave model in shallow water, which shows the generation and advancement of internal solitons in the ocean. From the figure, we see that the upper layer of density ρ_1 and depth d_1 is separated by the lower layer of density $\rho_2>\rho_1$, and depth d_2. Typically, in the mid-latitude continental shelf water [15], L varies in the range 1-5 km, the amplitude or the maximum elevation of pycnocline, η_0 ranges from 0 - 30 m. From the horizontal view we see that the characteristic soliton packet width, w_p, has value 100 m, the packet wavelength ranges from 50 - 500 m, the packet crest height, H_p, changes in the range 0-30 km, and two successive inter-packet distance varies in the range 15-25 km. The velocity of the internal wave, ξ_{in}, is expressed as:

$$\xi_{in} = \sqrt{\frac{g(\rho_2 - \rho_1)}{2(\rho_2 + \rho_1)(d_1 + d_2)}} \tag{15}$$

The situation becomes different when solitons propagate through a medium having arbitrary stratification. In this case, Korteweg-de Vries introduced a new analytical solution [15] for internal soliton. Let us consider the situation where internal solitons propagate through arbitrarily stratified medium with no rotation, i.e., the Coriolis parameter, f_c, is zero.

Under small dispersion and small non-linearity, the quadratic Korteweg-de Vries equation for internal waves propagating along the +x direction is expressed as [37], [38], [39]:

$$\frac{\partial \eta}{\partial t} + \xi_{in}\frac{\partial \eta}{\partial x} + \mu_1\eta\frac{\partial \eta}{\partial x} + \mu_2\frac{\partial^3 \eta}{\partial x^3} \tag{16}$$

In Equation (16), the constant quantities, μ_1 and μ_2 are expressed as:

$$\mu_1 = \frac{3\xi_{in}\varrho}{2\chi} \tag{17}$$

$$\mu_2 = \frac{\xi_{in}e_p\chi^2}{2} \tag{18}$$

DOI: 10.1002/dac

In Equations (17) and (18), the parameters ϱ and e_p are non-dimensional environmental parameters. The solution of Equation (16) is follows as [40]:

$$\eta(x,t) = \eta_0 sech^2(\frac{x - Vt}{\Delta}) \tag{19}$$

This solution is alternatively known as the "SECH" solution. In Equation (19), V is the non-linear speed of soliton, and Δ is the characteristic width. The parameters V and Δ can, respectively, be expressed in terms of μ_1 and μ_2 as:

$$V = \xi_{in} + \frac{\mu_1 \eta_0}{3} \tag{20}$$

$$\Delta^2 = \frac{12\mu_2}{\mu_1 \eta_0} \tag{21}$$

In Equation (23), μ_2 represents the positive oceanic gravity waves. However, in the shallow sea, with strong mixing, μ_1 and μ_2 are positive. From Figure 1, we write the expressions for μ_1 and μ_2 as follows:

$$\mu_1 = \frac{3}{2}\xi_{in}\frac{d_1 - d_2}{d_1 d_2},\ for\ 0 > z > -d_1 \tag{22}$$

$$\mu_2 = \frac{\xi_{in} d_1 d_2}{6},\ for\ -d_1 > z > -D \tag{23}$$

4. NETWORK ARCHITECTURE

In this paper, we have considered the shallow water oceanic coastal region. In this region, the nodes are deployed in such a manner that the sink nodes float on the water surface, and the other nodes stay at the sea-bed. We have considered single hop communication, i.e., the source nodes at the sea-bed directly communicate with the surface sink. The source nodes are equipped with long range acoustic transceiver, whereas the surface sinks are equipped with both acoustic and RF transceivers. The communication architecture is shown in Figure 1.
The following assumptions are made in this work.

- The deployed nodes are homogeneous in nature.
- The nodes in the sea-bed span an area covering the maximum transmission range of a node.
- The nodes have the capability of directional transmission.
- The sink nodes can be stationary as well as mobile.
- Mutual acoustical interference among the source nodes is negligible.

However, regarding communication, two issues may arise. One issue is the bandwidth decrement of acoustic signal during propagation through the channel. Another is the node's mobility for which Doppler effect results. Bandwidth problem is minimized to some extent at the receiving end. As a sensor node has the capability of amplification, the destination node will amplify the received signal. As the source and destination nodes are not affected by solitons, there is a less probability of arising Doppler effect.

5. PROPAGATION OF WIRELESS ACOUSTIC SIGNAL THROUGH INTERNAL SOLITON

The internal solitons strongly scatter the underwater sound signal, and this scattering has strong dependency on the frequency, f, of the signal used. Internal solitons mainly affect three frequency bands [15], which are given in Table I.

It is yet an open research problem to the researchers that particularly which of the tracers in the internal wave scatters acoustic signal. In this paper, we have assumed that sediment carried out by internal solitons is the tracer responsible for scattering of acoustic signal. In shallow water,

DOI: 10.1002/dac

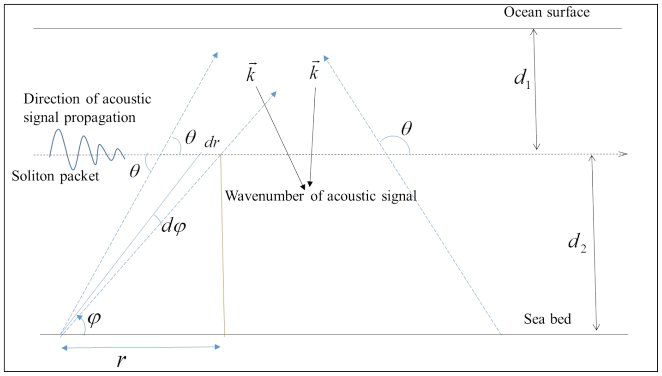

(a) Signal propagation through internal solitons

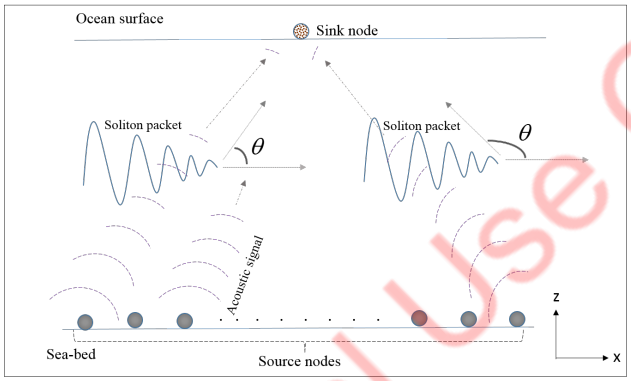

(b) Network architecture of UWASNs

Figure 2. Signal propagation through internal solitons

Table I. Acoustic frequency ranges through internal solitons

Frequency band	**Frequency range**
High frequency	f $\geq$ 50 kHz
Mid frequency	1 kHz $\leq$f $\leq$ 50 kHz
Low frequency	f $\leq$ 1 kHz

signal of frequency of the order of few hundred Hertz (Hz) faces less attenuation [15]. However, the optimum operating frequency of UWASNs lies in the range of few kHz, thereby increasing the signal attenuation. Interaction of acoustic signal with solitons leads to fluctuation in intensity, I, and pulse travel time, τ. Along with, I and τ, the signal attenuation affects " amplitude" and "phase".

5.1. Problem formulation for signal field calculation

An internal soliton makes changes to the medium properties along its direction. Therefore, the range dependent Helmholtz equation is written as [41]:

$$\nabla^2\Psi(r,z) + \kappa^2\Psi(r,z) = 0 \tag{24}$$

In Equation (24), r is the range, $\Psi(r,z)$ is the range and depth (z) dependent scalar function, and $\kappa(r,z) = \frac{\omega}{C(r,z)}$ is the wavenumber of the propagating acoustic signal, which also signifies the range dependent properties of a wave propagating through the medium. Using the method of partial

DOI: 10.1002/dac

separation of variables, the scalar function $\Psi(r,z)$ is expressed as [41]:

$$\Psi(r,z) = \sum_m \Re_m(r)\Phi_m(r,z) \tag{25}$$

In Equation (25), the parameter, $\Re$, is known as the radial part, which depends only on the range, r, and the function, Ψ depends both on range, r, and depth, z. Substituting Ψ from Equation (25) into Equation (24), we have the following modal equation:

$$\{\frac{\partial^2}{\partial z^2}\Phi_m(r,z)\} + (k^2 - k_m^2)\Phi_m(r,z) = 0 \tag{26}$$

The coupled mode equations for an acoustic wave in terms of the radial part, $\Re$, is written as [41]:

$$\frac{\partial^2 \Re_l}{\partial r^2} + r^{-1}\frac{\partial \Re}{\partial r} + k_l^2 \Re_l + \sum_l \{\Re_l(C_{ml} + \frac{D_{ml}}{r}) + 2D_{ml}\frac{\partial \Re}{\partial r}\} \tag{27}$$

In Equation (27), the parameters, C_{ml} and D_{ml}, are the mode-coupling co-efficients, and are functions of the density, $\rho(z)$, and the eigen function Φ.

We get the adiabatic mode solution corresponding to the single mode from coupled mode equations by setting the co-efficients, C_{ml} and D_{ml}, to zero, for acoustic field propagating along the internal wavefront as:

$$p(r,z) = (\frac{2\pi}{r})^{\frac{1}{2}} e^{i\frac{\pi}{4}} A(r,z)\Theta(r)\delta(r) \tag{28}$$

In Equation (28), A is the amplitude of signal, Θ is the phase, and the signal attenuation is accounted by the parameter, δ. The aforementioned parameters are presented as follows:

$$A(r,z) = \frac{\Phi(z_s)\Phi(z_r)}{\sqrt{\int_0^r k(r)\,dr}} \tag{29}$$

$$\Theta(r) = e^{i\int_0^r k(r)\,dr} \tag{30}$$

$$\delta(r) = e^{-\int_0^r \alpha(r)\,dr} \tag{31}$$

where, r is the range of a sensor node over which communication takes place.

5.2. *Modeling amplitude and attenuation co-efficient of wireless signal*

In general, any wave is associated with two fundamental properties: *amplitude* and *phase*. During propagation through internal soliton, the amplitude and phase of an acoustic signal get modified. In this section, we have modeled the amplitude and phase of an acoustic signal propagating through a medium consisting of internal solitons.

Amplitude:

The analysis in Section 5.1 for an acoustic field $p(r,z)$ is valid when signal propagation takes place across the soliton wavefront. However, as evident from the Figure 1, the propagating acoustic signal makes angles with the propagation direction of an internal soliton. The schematic representation of the scenario is shown in Figure 2. From the figure, we observe that the wavenumber makes an angle θ with the propagation direction of the soliton. So, the component of the wavenumber along the

DOI: 10.1002/dac

direction of propagation of solitons is $|\vec{k}|cos\theta$. Therefore, the integral,

$$\lceil = \int_0^r \frac{k}{r}\, dr \tag{32}$$

$$= \int_0^{tan^{-1}(D/r)} (\frac{2\pi f}{C_0})cot\theta.\frac{d\theta}{D}.tan\theta \tag{33}$$

$$= (f/C_0) \int_0^{tan^{-1}(D/r)} d\theta \tag{34}$$

We calculate the eigen functions, $\Phi(z_s)$ and $\Phi(z_r)$. For source depth, z_s, of 200 m and receiver at the surface, i.e., $z_r = 0\, m$, the eigen functions are expressed as:

$$\Phi(z_s) = cos(\frac{\pi \times D}{D}) = -1 \tag{35}$$

$$\Phi(z_r) = cos(\frac{\pi \times 0}{D}) = 1 \tag{36}$$

Therefore, the numerical value of phase, A, is expressed as:

$$A = \frac{1}{\frac{f}{C_0} \int_0^{tan^{-1}\frac{D}{r}} d\theta} \tag{37}$$

$$\tag{38}$$

Attenuation coefficient:
During the propagation of acoustic signal through internal solitons, scattering of signals occurs. This scattering occurs due to the interaction of signal with suspended sediments carried by waves. We have considered sand as the major contributor to sediments. We have assumed that there is a homogeneous suspension of sphere of radius R_s, and we have adopted the sphere scattering model. The attenuation co-efficient due to scattering with the internal wave is expressed as [42]:

$$\alpha = \frac{3M}{4R_s\rho_s}\chi(k) \tag{39}$$

In Equation (39), M is mass concentration of suspended sediment, ρ_s is the density of suspended particles, whose value is taken as 2650 $kg - m^s$ [43], R_s is the dimension of the suspended particles, and χ is the normalized total scattering. We have considered four sets of frequencies, viz., 20 kHz, 30 kHz, 40 kHz, and 50 kHz, and four sets of radii for suspended sediment, which are $-$ 100 μm, 150 μm, and 200 μm. The calculation of wavelength shows that the wavelength of the propagating acoustic wave is substantially greater than the circumferential length of the suspended particles. Therefore, scattering falls in the Rayleigh regime. For Rayleigh scattering, the function, χ, can be expressed as [44]:

$$\chi = 2x^4[\frac{e-1}{3e} + \frac{g-1}{2g+1}] \tag{40}$$

In Equation (40), $x = kR_s$, $e = 39$ is the ratio of elasticity of sand grains to water, g is the ratio of density of the sand grains to water. Substituting the values of e and g, we get the final equation of χ as:

$$\chi = 0.26x^4$$

$$\chi = \frac{0.26 \times 16\pi^4}{c^4}(fR_s)^4 \tag{41}$$

DOI: 10.1002/dac

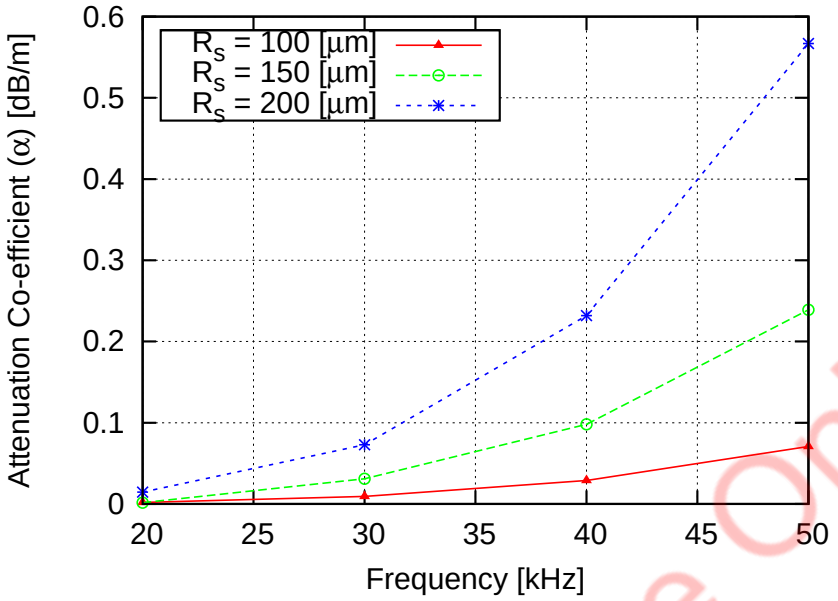

Figure 3. Variation of attenuation co-efficient

The variation of attenuation co-efficient for different frequencies under different particle sizes is shown in the Figure 3

As the intensity of scattering mainly depends on the particle size, and the frequency of acoustic signal, we have observed attenuation co-efficient for different particle sizes and variable frequencies. Therefore, the intensity of the acoustic signal is expressed as:

Table II. Scattering parameter and attenuation co-efficient of signal for different particle's size

R_s (μm)	f (kHz)	χ	α
100	20	0.0013×10^{-6}	0.0018×10^{-6}
	30	0.0065×10^{-6}	0.0092×10^{-6}
	40	0.0021×10^{-6}	0.0290×10^{-6}
	50	0.0500×10^{-6}	0.0708×10^{-6}
150	20	0.0065×10^{-6}	0.0061×10^{-6}
	30	0.0328×10^{-6}	0.0310×10^{-6}
	40	0.1037×10^{-6}	0.0980×10^{-6}
	50	0.2533×10^{-6}	0.2390×10^{-6}
200	20	0.0205×10^{-6}	0.0145×10^{-6}
	30	0.0137×10^{-6}	0.0730×10^{-6}
	40	0.3279×10^{-6}	0.2320×10^{-6}
	50	0.8004×10^{-6}	0.5670×10^{-6}

$$I_n = p.p^* \tag{42}$$

$$= \frac{C_0}{f} \frac{1}{\int_0^{\frac{f}{C_0}} tan^{-1}\frac{D}{r}\, d\theta} . \exp(-\alpha . \frac{100}{sin^2\theta}) \tag{43}$$

$$= \frac{C_0}{f} \frac{sin\theta}{D} . \exp(-\alpha . \frac{100}{sin^2\theta}) \tag{44}$$

DOI: 10.1002/dac

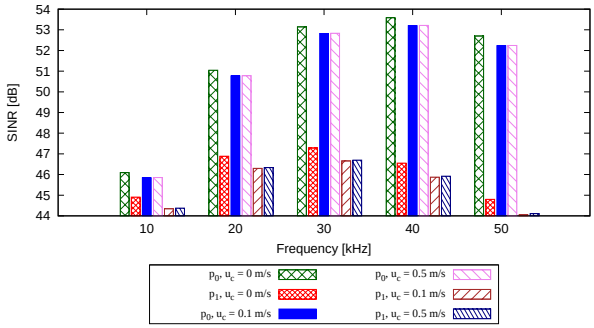

(a) SINR for data rate 500 bps

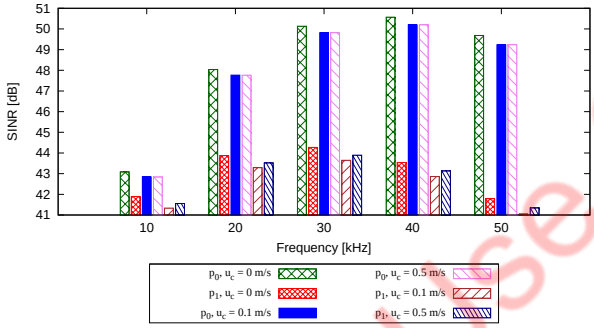

(b) SINR for data rate 1000 bps

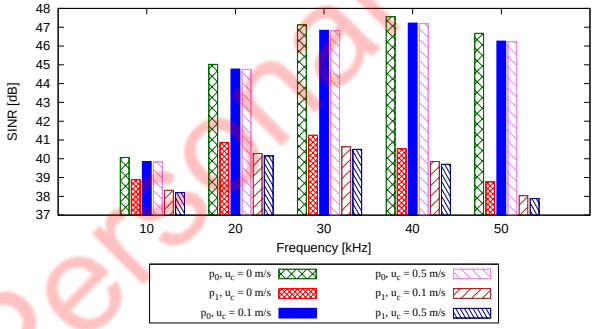

(c) SINR for data rate 2000 bps

Figure 4. Variation of SINR in presence of internal soliton

Finally, the transmission loss of a propagating signal is given as:

$$TL = -10\,log|I_n| \tag{45}$$

6. PERFORMANCE EVALUATION

In this section, we have analyzed the performance of UWASNs in the presence of internal solitons with respect to different metrics.

6.1. Simulation scenario

The simulation parameters are listed in Table III. We have taken a simulation region of dimension $100m \times 200m$. The sink node is placed on the sea surface and the source nodes are deployed on

the ocean bed. The 'meandering current mobility model' [45] was used to simulate mobility. This is the only UWSN mobility model available in the literature. Simulation was undertaken for node velocities of 0.1 m/s and 0.5 m/s. We adopted the 'ambient noise model' [46] as the noise model. Data rates of 500 bps, 1000 bps, and 2000 bps were considered. For communication between the source and the sink nodes, five sets of frequencies, 10 kHz, 20 kHz, 30 kHz, 40 kHz, and 50 kHz were taken into consideration. Data packets were sent from the source node to the sink node in an equal time interval of 10 seconds. The NS-3 simulator was used for simulation purpose.

Table III. Simulation Parameters

Parameters	**Values**
Deployment Region	$100m \times 200m$
Signal frequencies	10 kHz, 20 kHz, 30 kHz, 40 kHz, 50 kHz
Data rate	500 bps, 1000 bps, 2000 bps
Packet interval	10 sec
Mobility model	meandering current
Noise model	ambient noise model
Meandering current (u_c)	0.1 m/s, 0.5 m/s
Modulation scheme	64-QAM
Number of nodes (N)	100

6.2. *Performance metrics*

The following metrics were used for performance evaluation.

Signal-to-Interference-Plus-Noise-Ratio (*SINR*): It is used to estimate the node-to-node link quality. Interference occurs when multiple eigen rays interact with one another during propagation through a channel. Noise is channel's property added with the desired propagating signal. SINR is defined as the ratio between the desired signal and added value of interference and noise.

Bit Error Rate (*BER*): BER is a key parameter for the analysis of a system where digital data is sent from one point to another. During data transmission through the channel, there is a probability of error being introduced over transmitter, receiver, and the channel altogether. BER, typically, depends on interference, state of transmitter's power, and bandwidth. BER is defined as the ratio of the number of error bits and the total numbers of bits sent.

Delay: Defined as the time taken by the data packet to reach the sink node from the source node. In underwater environment, end-to-end delay is high [47].

Enery: The nodes consume energy in transmitting data from the source to the sink nodes. In our work, we have considered this metric as the amount of energy consumed per node in communicating with one another through the underwater channel.

6.3. *Benchmark*

We have compared our simulated result with the existing Thorp [48] propagation model applicable to ideal underwater oceanic environment. This model presents a practical scenario giving the frequency dependent sound attenuation in oceanic underwater channel. This model takes into account acoustic signal attenuation due to ocean water only. Phenomenon other than the channel are not considered for the calculation of attenuation. Therefore, in such a scenario, the performance of the overall network depends only on the channel property. In our case, we have considered the internal soliton as an additional phenomenon dominating the channel. As the Thorp model considers the case of ideal channel scenario, and ours considers the case of channel induced by internal soliton, we have taken the Thorp model as the benchmark for performance comparison. In this work, we measure the performance variation when the channel switches from ideal channel in Thorp to the internal soliton induced one.

DOI: 10.1002/dac

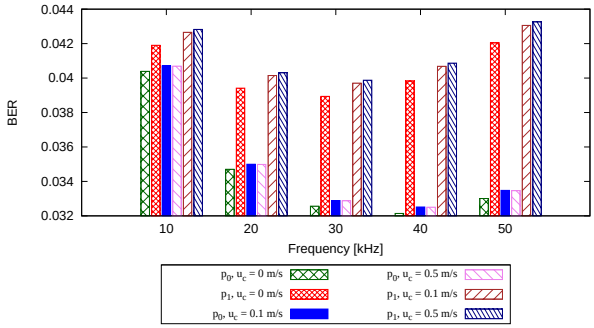

(a) BER for data rate 500 bps

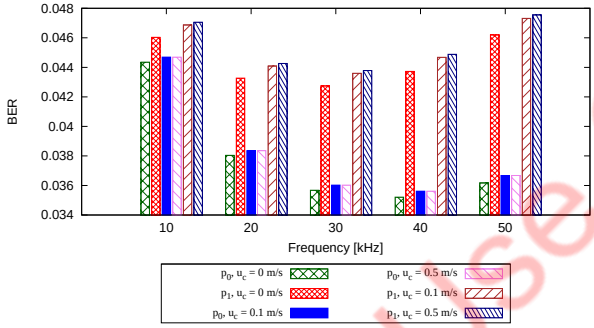

(b) BER for data rate 1000 bps

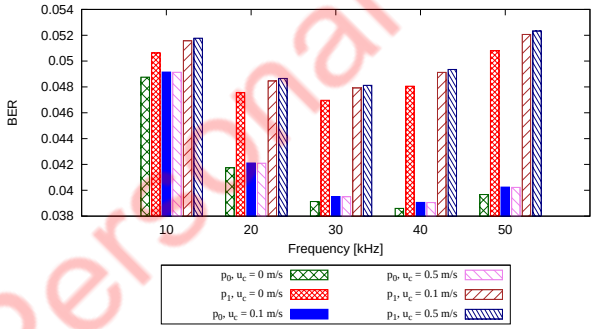

(c) BER for data rate 2000 bps

Figure 5. Variation of BER in the presence of internal solitons

6.4. *Result and discussion*

The results obtained with respect to the three metrics are given below. The results were compared with the results obtained using Thorp. To denote the Thorp scenario, we have used the notation p_0, and to signify the internal wave induced scenario, we have used the notation p_1.

6.4.1. SINR Figure 4 shows the variation of SINR with frequency under variable data rates. We observe from the figures that irrespective of whether the nodes are static or dynamic, the SINR values for Thorp are always more than the internal wave induced one. A close observation reveals that with the increase in data rate, SINR decreases. This is due to the fact that as the data rate increases, the probability of occurrence of interference increases, and at the same time more data will be associated with noise. It is seen from the figure that SINR in the static state is higher than in the dynamic state. With the increase in the mobility of nodes, SINR decreases. Additionally, we

DOI: 10.1002/dac

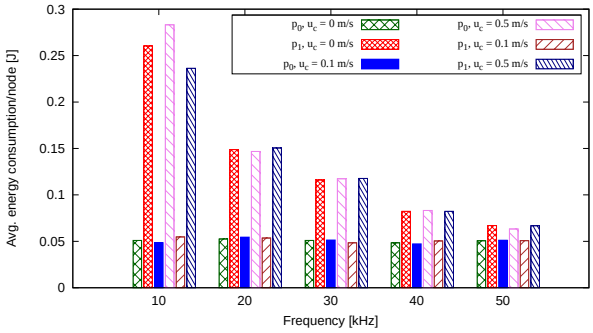

(a) Avg. energy consumption/node for data rate 500 bps

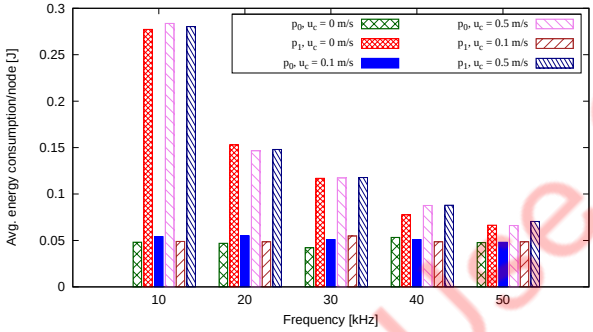

(b) Avg. energy consumption/node for data rate 1000 bps

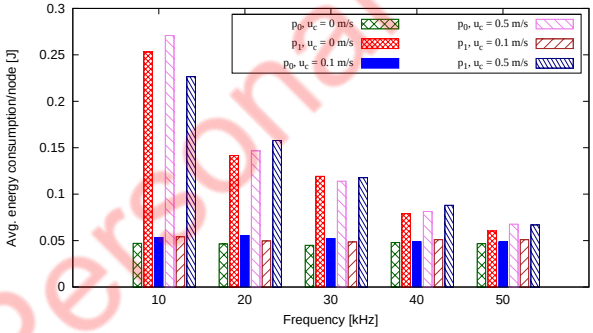

(c) Averageg energy consumption/node for data rate 2000 bps

Figure 6. Variation of average energy consumption/node in the presence of internal solitons

see from the figure that with the increase in frequency, SINR increases gradually at first and then decreases monotonically. This is due to the fact that with the increase in frequency, the attenuation of sound also increases. So, even an addition of a noise of low intensity with low intensity sound decreases the SINR. We see from the figure that, as compared to the dynamic node, the rate of decrease of SINR with the increase in frequency is lower in case of static nodes under the Thorp scenario. For the static scenario, the value SINR using the Thorp model increases by 9.35 % for static situation of the nodes, and by 9.79 %, when the nodes are mobile.

6.4.2. BER Figure 5 shows the plot of BER for different frequencies for different data rates. From the figure, we observe that BER for the Thorp model is always higher than the internal soliton induced channel model. We infer that as compared to the data rate of 1000 bps and 2000 bps, BER decreases rapidly with the increase in frequency for data rate of 500 bps. This is due to the fact that for low data rate the volume of data sent per unit time is less, and therefore, less data is available

DOI: 10.1002/dac

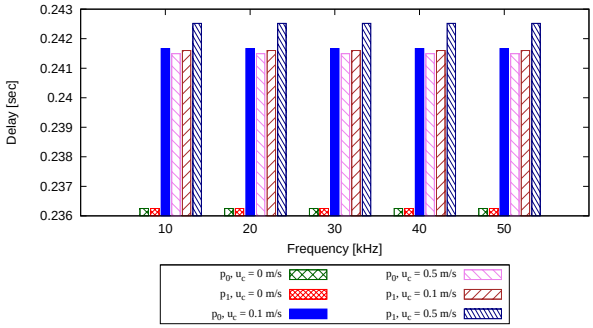

(a) Delay for data rate 500 bps

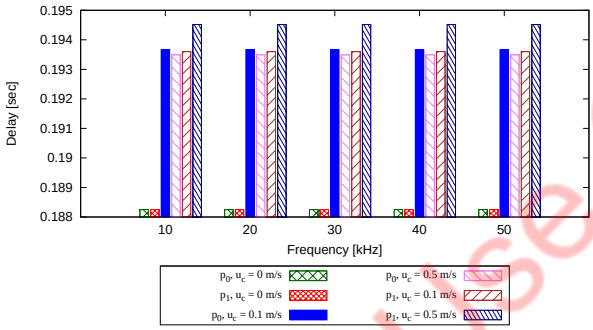

(b) Delay for data rate 1000 bps

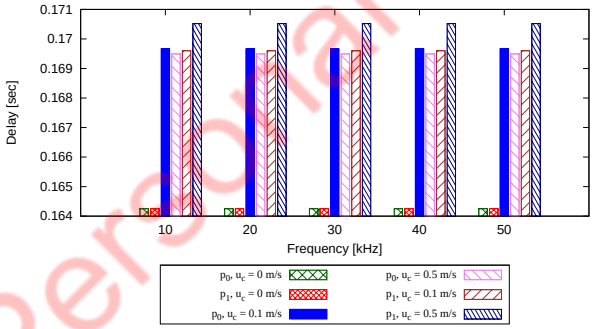

(c) Delay for data rate 2000 bps

Figure 7. Variation of delay in the presence of internal solitons

for getting corrupted. On the other hand for the internal soliton induced case, there is no significant decrease in BER. The high BER is due to the interaction of acoustic signal with the internal soliton. We see from the figure that BER gradually decreases upto 30 kHz, and then again increases upto 50 kHz. This is because with the same data rate, when frequency increases, the volume of data passing between the intermediate nodes becomes faster, as a result of which the interaction of data with channel increases. Again we see that when the mobility of nodes increases, the BER increases. When a moving node transmits data to its neighbor, the probability of corruption of data increases. Analytically it can be shown that in the presence of internal solitons, BER increases by 15.76 % for static nodes, and 17.21 % when the nodes are.

6.4.3. Delay Figure 7 shows the variation in delay with respect to frequency under variable data rates. From the figure, it is obvious that the time taken by a stationary source node to transmit data to sink nodes is much less than the time taken by the mobile source nodes. However, in the presence

DOI: 10.1002/dac

of solitons, delay is more than in the absence of it. However, the delay profiles under the static situation of the nodes are almost similar for all the data rates. It can be inferred that the travel time does not depend on data rate. It depends on the frequency of the signal used and the kinematics of the nodes. On an average, the delay for the moving nodes increases by 0.24 % in the presence of internal solitons.

6.4.4. Energy Figure 6 shows the average energy consumed by each of the nodes due to communication. When the nodes are in the static mode, the energy consumption is more in the presence of internal soliton than using using the Thorp model. When the nodes move with the meandering current, they consume more energy. Again, we observe from the figure that compared to the case using Thorp, the nodes consume more energy than in the internal soliton induced region. Numerically, we can infer that in the presence of internal solitons, the energy consumption per node under static situation increases by 53.31 % and 52.78 % for the moving nodes.

7. CONCLUSION

Our study focuses on the performance analysis of distributed UWASNs in the presence of internal solitons. The study was performed in the shallow coastal region of the ocean. To simulate the environment, we used NS-3 simulator. We took 200 m depth of the simulation region. We have analyzed the performance of UWASNs in terms of some performance metrics, viz., SINR, BER, delay, and energy consumption per node. These metrics are observed to be affected by the presence of internal solitons. To calculate transmission loss, we have calculated the intensity of acoustic signal propagating through internal wave.

Based on the analysis, it is observed that in presence of internal solitons, SINR decreases by 9.57 % and BER increases by 16.49 %, delay increases by 0.24 %, and energy consumption per node increases by 53.05 %. in the future, we plan to perform similar studies with other oceanic phenomena such as the effects of rain drops on near-surface oceanic environments. Following the present analytical and simulation based studies, we also plan to perform real-life field-test experiments in the future.

REFERENCES

1. Watfa MK, Selman S, Denkilkian H. Uw-mac: An underwater sensor network mac protocol. *International Journal of Communication Systems* 12^{th} March 2010; **23**:485–506.
2. Wahid A, Lee S, Kim D. A reliable and energy-efficient routing protocol for underwater wireless sensor networks. *Internation Journal of Communication Systems* 11^{th} October 2012; .
3. Obaidat MS, Misra S. *Principles of wireless sensor networks*. Cambridge University Press, 2014.
4. Dhurandher SK, Obaidat MS, Gupta M. An efficient technique for geocast region holes in underwater sensor networks and its performance evaluation. *Simulation: Modeling Practice and Theory* September 2011; **19**(9):2102–2116.
5. Akyildiz IF, Pompili D. Underwater acoustic sensor network: Research challenges. *Ad Hoc Networks* February 2005; **3**(3):257–279.
6. Heidemann J, Stojanovic M. Underwater sensor networks: applications, advances and challenges. *Philosophical Transactions of the Royal Society* August 2012; **370**:158175.
7. Heidemann J, Mitra U, Preisig J, Stojanovic M, Zorzi M. Underwater wireless communication networks. *IEEE Journal of Selected Areas in Communication* December 2008; **26**(9):16171619.
8. Erol-Kantarci M, Mouftah HT, Oktug S. A survey of architectures and localization techniques for underwater acoustic sensor networks. *IEEE Communications Surveys and Tutorials* March 2011; **13**(3):487–502.
9. Nicopolitidis P, Christidis K, Papadimitriou G, Sarigiannidis PG, Pomportsis AS. Performance evaluation of acoustic underwater data broadcasting exploiting the bandwidth-distance relationship. *Jounal of Mobile Information Systems* 7^{th} November 2011; **7**(4):285–298.
10. Erol-Kantarci M, Oktug SF, Filipe L, Vieira M, Gerla M. Performance evaluation of distributed localization techniques for mobile underwater acoustic sensor networks. *Ad Hoc Networks* 2011; **9**(1):61–72.
11. Erol-Kantarci M, Mouftah HT, Oktug SF. Localization techniques for underwater acoustic sensor networks. *IEEE Communications Magazine* 2010; **48**(12):152–158.
12. Misra S, Dash S, Khatua M, Vasilakos A, Obaidat M. Jamming in underwater sensor networks: detection and mitigation. *IET Communications* 2012; **6**(14):2178–2188.

13. Dhurandher SK, Obaidat MS, Gupta M. A novel geocast technique with hole detection in underwater sensor networks. *Proceedings of ACS/IEEE International Conference on Computers and Applications*, Hamammet, Tunisia, 2010.
14. Dhurandher S, Obaidat MS, Goel S, Gupta A. Optimizing energy through parabola based routing in underwater sensor networks. *Proceedings of the IEEE GLOBECOM 2011 - Communications QoS, Reliability, and Modeling Symposium*, 2011.
15. Apel JR, Ostrovsky LA, Stephanyants YA, Lynch JF. Internal solitons in the ocean and their effect on underwater sound. *Journal of Acoustical Society of America* February 2007; **121**(2):695–722.
16. Kostin A, Oz G, Haci H. Performance study of a wireless mobile ad-hoc network with orientation dependent internode communication scheme. *International Journal of Communication Systems* 17^{th} January 2014; **27**:322–340.
17. Chang LW, Huang YM, Lin CC. Performance analysis of S-MAC protocol. *International Journal of Communication Systems* 23^{rd} 2013; **26**:1129–1142.
18. Kulakowski P, Calle E, Marzo JL. Performance study of wireless sensor and actuator networks in forest fire scenarios. *International Journal of Communication Systems* 12^{th} March 2013; **26**:515–529.
19. Proakis JG, Sozer EM, Rice JA, Stojanovic M. Shallow water acoustic networks. *IEEE Communications Magazine* November 2001; :114–119.
20. Kuperman WA, Lynch JF. Shallow water acoustics. *Physics Today* October 2004; :55–61.
21. Climent S, Capella JV, Meratnia N, Serrano JJ. Underwater sensor networks: a new energy efficient and robust architecture. *Journal of Sensors* 9^{th} January 2012; **12**(1):704–731.
22. Real G, Beaujean PP, Bouvet PJ. MIMO underwater acoustic communications in ports and shallow waters at very high frequency. *Journal of Sensor and Actuator Networks* 2013; **2**:700–716.
23. Ismail NSN, Hussein LA, Ariffin SHS. Analyzing the performance of acoustic channel in underwater wireless sensor. *Proceedings of IEEE International Conference on Mathematical/Analytical Modelling and Computer Simulation*, Kota Kinabalu, Malaysia, 2010; 550–555.
24. Zorzi M, Baldo N. Energy-efficient routing schemes for underwater acoustic networks. *IEEE Journal on Selected Areas In Communication* December 2008; **26**(9):1754–1766.
25. Stefanov A, Stojanovic M. Design and performance analysis of underwater acoustic networks. *IEEE Journal of Oceanic Engineering* December 2011; **29**(10):2012–2021.
26. Babu AV, Joshy S. Maximizing the data transmission rate of a co-operative relay system in an underwater acoustic channel. *International Journal of Communication Systems* 25^{th} January 2012; **25**:231–253.
27. Xu M, Liu G, Wu H, Sun W. Towards robust routing in three-dimensional underwater wireless sensor networks. *International Journal of Distributed Sensor Networks* 1^{st} October 2013; **2013**:1–15.
28. Ancy SB, Hammed SS. Energy efficient and reliable communication in underwater acoustic sensor networks. *International Journal of Advanced Research in Computer Engineering & Technology (IJARCET)* January 2013; **2**(1):169–173.
29. Llor J, Malumbres MP. Statistical modeling of large-scale signal path loss in underwater acoustic networks. *Journal of Sensors* 7^{th} February 2013; **13**:2279–2294.
30. Xie G, Gibson J, Gonzalez LD. Incorporating realistic acoustic propagation models in simulation of underwater acoustic networks: a statistical approach. *Proceedings of MTS/IEEE Oceans*, Boston, 2006; 1–9.
31. Apel JR. *Oceanic internal wave and solitons*, chap. 7. Global ocean associates, silver spring, maryland, usa, 2000.
32. Filonov A, Novotryasov V. On a spectrum of nonlinear internal waves in the oceanic coastal zone. *Nonlinear Processes in Geophysics* 13^{th} November 2007; **14**:757–762.
33. Zhou J, Zhang X, Rogers PH. Resonant interaction of sound wave with internal solitons in the coastal zone. *Journal of Acoustical Society of America* 30 May 1991; **90**:2042–2054.
34. Pickard GL. *Introductory dynamical oceanography*. 2^{nd} edition edn., Butterworth-Heinemann, 1978.
35. LeBlond P. *Waves in the ocean*. Elsevier oceanography series, Distributors for the U.S. and Canada: Elsevier/North Holland, 1980.
36. Lynch JL, Jin G, Pawlowicz R. Acoustic travel time perturbations due to shallow water internal wave and internal tide in the barents sea polar front: theory and experiment. *Journal of Acoustical Society of America* 1999; **99**(2):2042–2054.
37. Whitham GB. *Linear and non-linear waves*. Wiley-Interscience, New York, 1974.
38. Miropolsky YZ. *Dynawave of internal gravity waves in the ocean*. Atmospheric and Oceanographic Science Library, Springer, 2001 edition, 2001.
39. Ablowitz MJ, Segur H. *Solitons and the inverse scattering transform*. Studies in Applied and Numerical Mathematics (Book 4), Society for Industrial and Applied Mathematics; 1st edition, 2000.
40. Cuihua L, Biao C, Ronghua T, Suqin X, Guoxing G. A model for acoustic fluctuations due yo internal waves. *Proceedings of IEEE 2nd International Conference on Signal Processing Systems (ICSPS)*, 2010; 747–751.
41. Jensen FB, Kuperman WA, Porter MB, Schmidt H. *Computational ocean acoustics*. Modern Acoustics and Signal Processing, American Institute of Physics, 1997.
42. Moatea BD, Thorne PD. Scattering from suspended sediments having different and mixed mineralogical compositions: comparison of laboratory measurements and theoretical predictions. *Journal of Acoustical Society of America* 4^{th} January 2013; **133**(3):1320–1334.
43. Meral R. Laboratory evaluation of acoustic backscatter and lisst methods for measurements of suspended sediments. *Journal of Sensors* 7^{th} February 2008; **8**:979–993.
44. Medwin H, Clay CS. *Fundamentals of Acoustical Oceanography*. 1^{st} edition edn., Applications of Modern Acoustics, Academic Press, 1997.
45. Caruso A, Paparella F, Filipe L, Vieira M, Erol M, Geria M. The meandering current mobility model and its impact on underwater mobile sensor networks. *Proceedings of IEEE INFOCOM*, Phoenix, AZ, 2008.
46. Harris AF, Zorzi M. Modeling the underwater acoustic channel in ns2. *Proceedings of the 2^{nd} international conference on Performance evaluation methodologies and tools*, Nantes, France, 2007.

47. Abdelkader T, Naik K, Nayak A, Goel N, Srivastava V. SGBR: A routing protocol for delay tolerant networks using social grouping. *IEEE Transactions on Parallel and Distributed Systems* December 2013; **24**(12):2472 2481.
48. Thorp WH. Analytic description of the low frequency attenuation coefficient. *Journal of Acoustical Society of America* 8^{th} March 1967; :270.

DOI: 10.1002/dac